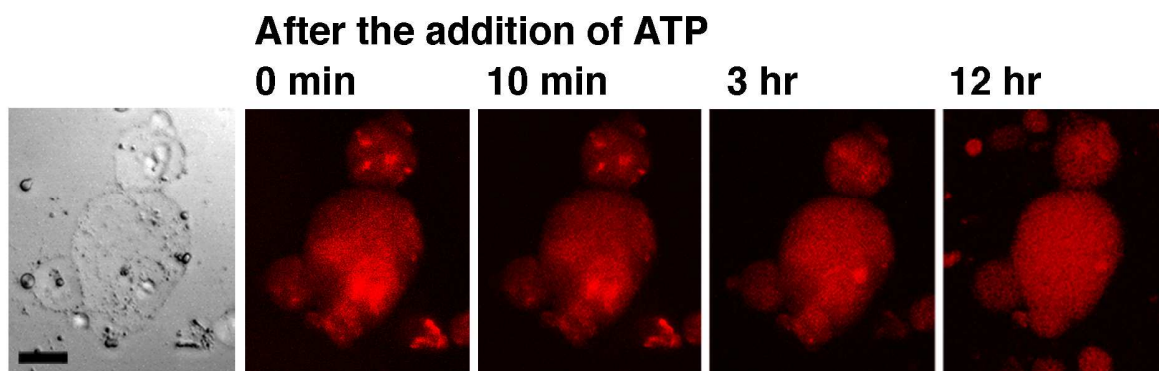


## Supporting Information

# Transformation of ActoHMM Assembly Confined in Cell-Sized Liposome

*Kingo Takiguchi,\*, † Makiko Negishi, ‡, § Yohko Tanaka-Takiguchi, † Michio Homma, † and  
Kenichi Yoshikawa\*, ‡*

†: Division of Biological Science, Graduate School of Science, Nagoya University, Furo-cho, Chikusa-ku, Nagoya 464-8602, Japan, ‡: Department of Physics, Graduate School of Science, Kyoto University, Sakyo-ku, Kyoto 606-8502, Japan, §: Current address: Department of Basic Science, Graduate School of Arts and Sciences, The University of Tokyo, Tokyo 153-8902, Japan.



**Figure S1.** Fluorescence images indicating the disassembly process of F-actin bundles formed with the co-encapsulated HMM. Confocal microscopic observation of the time-dependent changes in the distribution of actoHMM after the addition of ATP to the liposome (left image: transmission, other images: fluorescence). ActoHMM-encapsulating giant liposomes with a DOPC bilayer membrane were made using the spontaneous transfer method. The concentrations of encapsulated F-actin and HMM are 50 and 5.0  $\mu\text{M}$ , respectively. This Figure represents the larger neighboring area for the observation shown in Figure 2. F-actin is labeled with rhodamine-phalloidin. The time after the ATP supply through the added  $\alpha$ -hemolysin is indicated at the top of each panel. The sample was observed for 3 hr at 25°C, and then left for 12 hr at 4°C. The picture on the right was taken after adjusting the temperature back to 25°C. Bars = 20  $\mu\text{m}$ . Transmission images show the existence of small oil droplets around the liposome, which were squeezed out from the oil phase.<sup>1</sup>

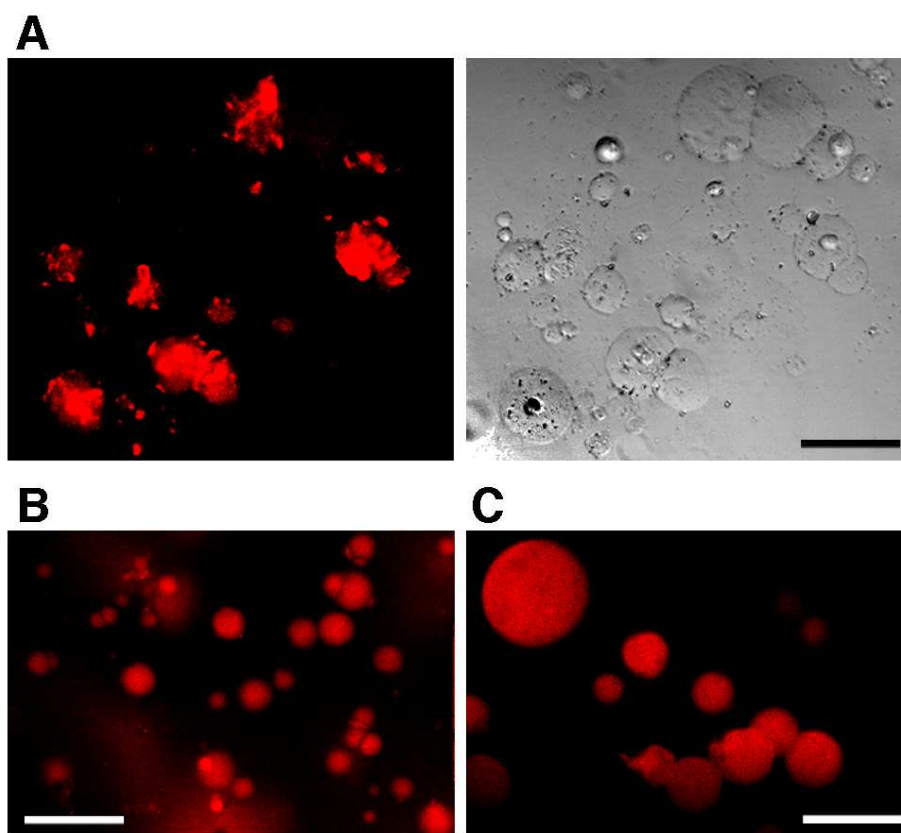


**Figure S2.** (A) Confocal microscopic images of actoHMM-encapsulating giant liposomes made from DOPC using the spontaneous transfer method (left: fluorescence, right: transmission).<sup>2</sup> The concentrations of encapsulated F-actin and HMM are 50 and 5.0  $\mu\text{M}$ , respectively. (B and C) Confocal microscopic images of giant liposomes encapsulating only F-actin (B) or actoS-1 (C) obtained using the spontaneous transfer method (fluorescence images). The concentrations of encapsulated F-actin and S-1 are 50 and 60  $\mu\text{M}$ , respectively. Fluorescence images show the distribution of rhodamine-phalloidin-labeled F-actin. Under these conditions, most liposomes are spherical and no protrusions develop. Bars = 100  $\mu\text{m}$ .

## Liposome entrapping mesh structure that is generated from asters

+ ATP

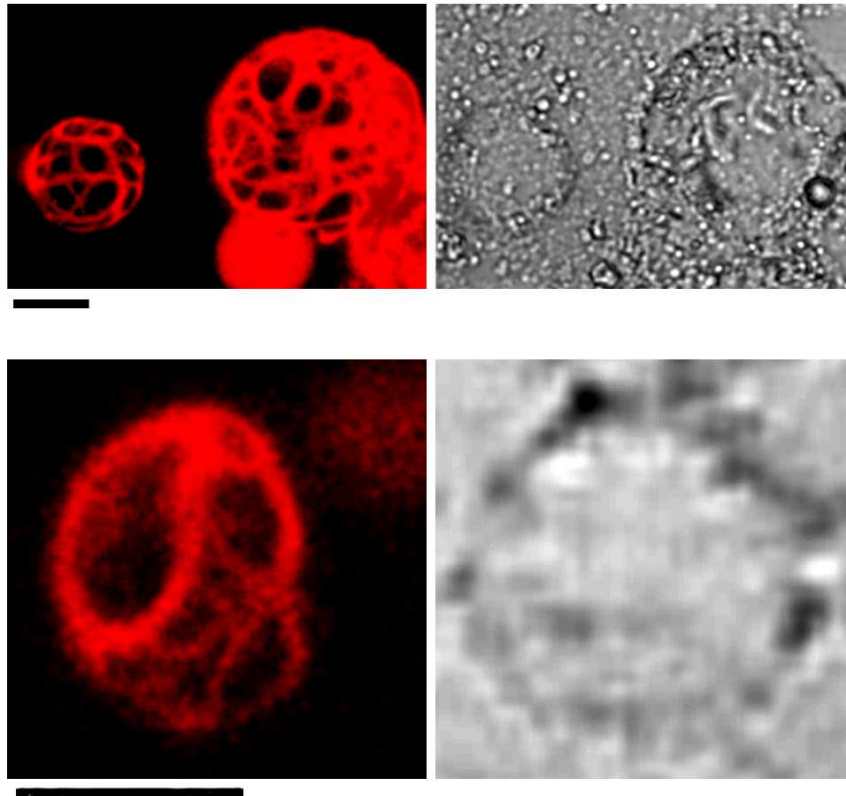


**Figure S3.** Giant liposomes that are entrapping an actoHMM mesh (left: fluorescence, right: transmission). The lipid composition was DOPC/DPPC/cholesterol. The concentrations of F-actin and HMM are 10 and 20  $\mu\text{M}$ , respectively. Bars indicate 20  $\mu\text{m}$ . Methylcellulose-formed actoHMM bundles are transformed to asters in the bulk solution by the addition of ATP. The asters are then encapsulated into cell-sized giant liposomes using the spontaneous transfer method after the pipetting procedure. By the suspension, the asters change in the mesh. ATP is supplied using treatment with  $\alpha$ -hemolysin as described in Material and Methods.

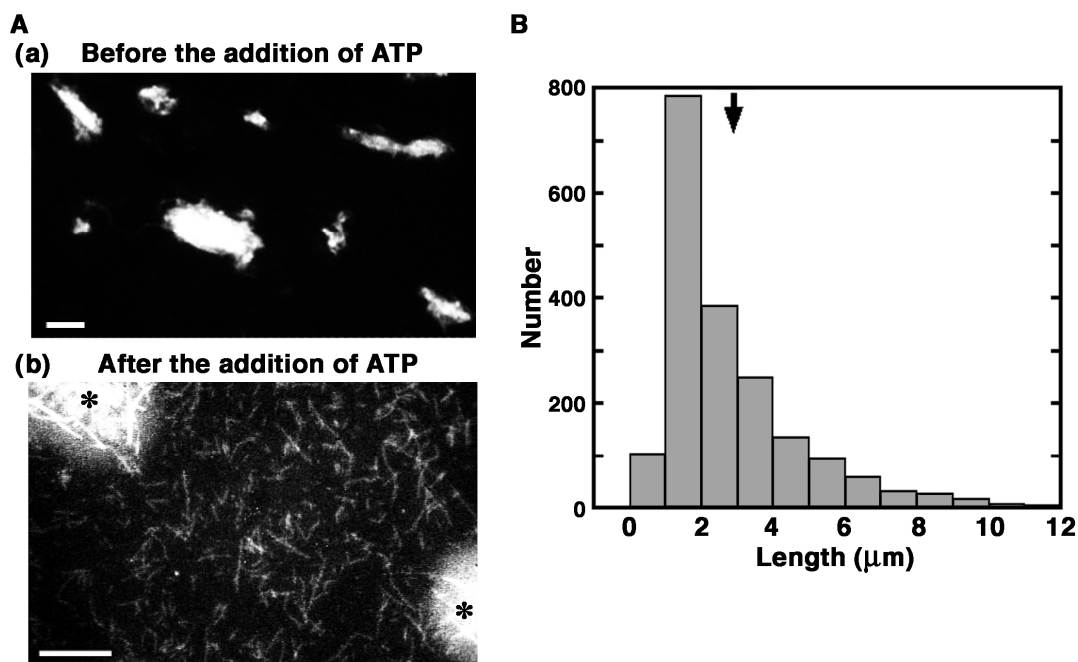


**Figure S4.** Length distribution of F-actin within bundles. (A) Actin bundles, which were prepared by the same procedure for the droplet formation in the oil, were attached to an HMM-coated glass surface (a). Subsequently, collapse of the bundles was observed by dark-field microscopy by the introduction of ATP. After the collapse of almost all of the bundles, debris of bundles was washed with the ATP-containing solution and then individual F-actin spread from bundles was observed by fluorescence microscopy and was measured length by use of ImageJ software (b). F-actin was labeled with rhodamine-phalloidin. Bars show 10  $\mu\text{m}$ . Asterisks indicate the remaining debris of bundles. (a) and (b) show the representative images of bundles before the addition of ATP (dark-field) and F-actins after the addition of ATP (fluorescence) on a glass surface, respectively. The concentrations of F-actin and HMM used were 10 and 20  $\mu\text{M}$ , respectively. (B) Histogram shows length distribution of F-actin within bundles ( $n=1,918$ ). Arrow indicates the average length (2.9  $\mu\text{m}$ ).

As shown in Figure S1, after the addition of  $\alpha$ -hemolysin and ATP, the crosslinked F-actins started to disassemble simultaneously inside many liposomes. Since the molecular weight of  $\alpha$ -hemolysin is 33 kDa, the simply estimated molar ratio of the heptamer of the pore-forming protein to lipid is roughly 1:20000 in our conditions (the concentrations of  $\alpha$ -hemolysin and lipid are 12.5  $\mu\text{g/ml}$  and 1 mM, respectively). If the occupied area of the lipid molecule in the monolayer is a fraction of square nanometers, a liposome with a radius of 10  $\mu\text{m}$  would be made from about  $1 \times 10^{10}$  lipids. Therefore, the number of pores that are opened in the liposomes by  $\alpha$ -hemolysin may be sufficient to supply ATP to the actoHMM that is encapsulated in the liposomes.

Figure S2 shows giant liposomes encapsulating F-actin (50  $\mu\text{M}$ ) and HMM (5.0  $\mu\text{M}$ ) in the presence of  $\text{MgCl}_2$ . The small spherical objects situated around the liposomes or on their surfaces in the transmission images are attributed to oil droplets at the oil/water interface.<sup>1</sup> Inside of those liposomes, F-actin co-encapsulated with HMM assembles into large bundles or networks (Figure S2A).<sup>2</sup> We have confirmed the appearance of similar assemblies of F-actin in an aqueous solution in control experiments. On the other hand, in the case of liposomes encapsulating the same concentration of F-actin only, F-actins inside the liposomes exist in a homogeneous manner (Figure S2B).<sup>2</sup> Moreover, giant liposomes co-encapsulating the same concentration of F-actin and S-1, instead of HMM, showed a uniform distribution of F-actin, even under conditions where an excess molar ratio of S-1 was co-encapsulated (Figure S2C).<sup>2</sup>

Myosins are classified into two groups according to their head-structure, *i.e.* double- or single-headed myosins. Myosins belonging to the double-headed type, such as myosin-II, and a

double-headed derivative of myosin-II, such as HMM, have frequently been studied as a representative double-headed myosin.<sup>3,4</sup> On the other hand, S-1 has often been studied as a representative simple single-headed myosin. S-1 has only one actin-binding motor domain and is unable to crosslink F-actins. Thus, these results indicate that the crosslinking of F-actins by the double-headed HMM is the motive force for organizing the actin bundles and networks.<sup>2</sup>

#### References for Supporting Information

- (1) Yamada, A.; Yamanaka, Y.; Hamada, T.; Hase, M.; Yoshikawa, K.; Baigl, D. *Langmuir* **2006**, *22*, 9824-9828.
- (2) Takiguchi, K.; Yamada, A.; Negishi, M.; Tanaka-Takiguchi, Y.; Yoshikawa, K. *Langmuir* **2008**, *24*, 11323-11326.
- (3) Takiguchi, K. *J. Biochem.* **1991**, *109*, 520-527.
- (4) Tanaka-Takiguchi, Y.; Kakei, T.; Tanimura, A.; Takagi, A.; Honda, M.; Hotani, H.; Takiguchi, K. *J. Mol. Biol.* **2004**, *341*, 467-476.